

The collider landscape: which collider for establishing the SM instability?

Roberto Franceschini,^a Alessandro Strumia^b and Andrea Wulzer^c

^a*Dipartimento di Matematica e Fisica, Università degli Studi di Roma Tre,
Via della Vasca Navale 84, 00146 Roma, Italy*

^b*Dipartimento di Fisica “E. Fermi”, Università di Pisa,
Largo B. Pontecorvo 3, 56127 Pisa, Italy*

^c*Dipartimento di Fisica e Astronomia, Università di Padova,
Via Marzolo 8, 35131 Padova, Italy*

E-mail: roberto.franceschini@uniroma3.it,
Alessandro.Strumia@unipi.it, wulzer@cern.ch

ABSTRACT: Capabilities of future colliders are usually discussed assuming specific hypothetical new physics. We consider the opposite possibility: that no new physics is accessible, and we want to learn if the unnatural Standard Model is part of a vast landscape. We argue that a main step in this direction would be establishing the possible instability scale of the Higgs potential. This primarily needs reducing the uncertainty on the strong coupling and on the top quark mass. We show that the top quark mass can be measured well enough via a $t\bar{t}$ threshold scan with low $10^{33} \text{ cm}^{-2}\text{sec}^{-1}$ luminosity, that seems achievable at a ‘small’ e^+e^- collider in the LEP tunnel, or at a muon collider demonstrator.

KEYWORDS: Hierarchy Problem, Higgs Properties, Other Weak Scale BSM Models, Top Quark

ARXIV EPRINT: [2203.17197](https://arxiv.org/abs/2203.17197)

Contents

1	Introduction	1
2	The SM vacuum (in)stability	4
3	A top threshold collider	8
4	Conclusions	15
A	Increasing the information content of known physics	16
A.1	General information-theory discussion	16
A.2	Practical physical discussion	19

1 Introduction

Exploring short-distance physics systematically and conclusively has always been the true motivation for building colliders. However it is a fact that recent past colliders have been instead justified by safe Standard Model (SM) targets (such as finding the Z , Higgs, or the top quark) and by often overemphasized Beyond the SM (BSM) targets. Maybe this happened because pure exploration is not considered a valid motivation for the community at large. In this case, no collider will be built in the medium-term future, nor any other large-scale enterprise will be initiated aimed at probing short-distance physics, because we exhausted the SM targets and because the most compelling BSM ideas have lost a good portion of their appeal and motivation.

If instead the quest for exploration will prevail, we will soon have to decide which collider or colliders to build, based on an unavoidably subjective assessment of the exploration potential of the different projects. The role of BSM theory in this context is to bring objective elements for the assessment by identifying possible BSM realities and quantifying the perspectives for probing them. For instance one might find interesting to establish if, or not, the observed Dark Matter abundance is due to the thermal freeze-out of an electroweak charged particle, and rank future colliders by the amount of progress they can make in answering this question. The ranking is objective, but in some cases it strongly depends on the question that is being asked, which is subjective. For instance, Dark Matter might be an electroweak multiplet with no strong interactions, or a strong multiplet with no electroweak interactions: very different colliders are needed in the two cases.

The need of studying capabilities of future colliders from multiple perspectives, in order to offer the most complete assessment possible of their exploration potential, is well-understood in the community. The focus so far has been on BSM models or scenarios that foresee new physics at accessible energies.

In this paper we consider instead the opposite possibility: that the apparent unnaturalness in the weak scale and in the cosmological constant originates from anthropic selection in a landscape of many vacua, possibly $N \sim 10^{500}$, populated by cosmological inflation [1–5]. In this context no new physics could exist up to inaccessibly high energies, possibly up to the Planck scale. The appeal of this plausible although vague interpretation resides in its radical conservatism (standard theory brought to its extreme consequences can explain why the vacuum energy and the weak scale seem unnatural), as opposed to conservative radicalism (invent unusual new theories arranged such that we do not see them yet).

Its limitation is the lack of predictions and of concrete implications. We might be able to tell whether the scenario is true only after getting access to the microscopic theory that generates the landscape of vacua, by means of experiments we have no idea how to build. The theory itself is not known, and definitely not unique. It seems realized in the string/ M -theory framework, although huge landscapes of vacua also arise in Quantum Field Theories with some hundreds of heavy scalars [6, 7].

No collider, nor any other type of experiment envisaged so far can falsify anthropic selection and the landscape. Still we can ask which collider would be the most useful from this unusual point of view. For this assessment we clearly have to depart from the usual practice of studying collider perspectives to discover or bound specific hypothetical new particles or interactions, since no new physics is needed at accessible energies in the scenario we are considering. Rephrasing in modern form the words sometimes attributed to Kelvin (*‘there is nothing new to be discovered in physics now. . . all that remains is more and more precise measurements’*) [8]:¹ maybe all that remains, for the near future, could be measuring the SM more and more precisely.

At the same time the landscape scenario provides a specific direction where this endeavour can have fundamental significance: *measuring more precisely the free parameters of the SM* that seem ‘fundamental’ because we do not understand their values. Before discussing what it means, let us tell what it does not mean. The following example of measurements, while being relevant from different perspectives, are not relevant from this perspective:

- Measuring the Higgs interactions to fermions adds nothing, as the fundamental parameters of the SM that control these interactions, the Higgs Yukawa couplings, are already more precisely measured from the fermion masses. The same applies to all the single Higgs couplings and to the trilinear coupling.
- Similar considerations can be made for the $g - 2$ of the muon and other very precise measurements that do not help determining the SM fundamental parameters.²

What becomes relevant according to this point of view is acquiring more information about the fundamental constants that act as ‘coordinates’ for the SM, if it lives in a landscape of $N \gg 1$ vacua. If a plausible theory will become available for the microscopic structure of the landscape of vacua, the augmented knowledge will help us locate the single

¹Kelvin’s statement illustrates that predicting the future is remarkably difficult.

²Needless to say, constants such as c, \hbar, k_B are now understood as arbitrary conversion units.

vacua we happen to live in, and in principle to identify it uniquely by asymptotically accurate measurements. Very roughly, if $N \sim 10^{500}$ we need to measure fundamental constants up to acquiring 500 digits of information. In appendix A we discuss how Conditional Entropy allows to quantify the required and the present amount of information. Depending on the structure of the landscape theory, specific strategic measurements add more information. Since this structure is presently unknown the discussion remains abstract: we do not presently know which measurements would have strategic significance. We reasonably guess that this happens for those parameters that happen to be close to a qualitative transition or anthropic selection boundary

A clear case are the parameters that control the possible existence of an extra minimum of the Higgs potential, that appears at field values much above the physical SM minimum where $\langle H \rangle = v = 174$ GeV. The existence or not of this second minimum is a qualitative feature of the SM extrapolated up to high energies, which provides structural information relevant for future attempts of deriving the SM as one vacuum of a deeper high-energy quantum-gravity theory. For instance, a negative Higgs quartic at the Planck scale might rule out entire classes of vacua, or conversely select them if a deeper vacuum is obliged to exist (no de Sitter conjecture, see e.g. section 5 of [9]).

The current measurements of the relevant parameters (namely, α_3 , M_h and M_t) favour the existence of a second SM minimum, but more precise determinations are needed for a conclusive assessment. Furthermore, if the second minimum exists, precise measurements will allow us to compute the height and the width of the potential barrier between the two minima, which in turn is relevant for the cosmological history of the universe, possibly associated with an anthropic selection boundary. In fact, it is non-trivial that the $\langle H \rangle = v$ minimum is selected during inflation, nor that it is preserved by reheating [9, 10]. The conditions for this to happen depend also on cosmological parameters, such as the Hubble scale during inflation and the reheating temperature. When the latter parameters will be also determined, precise measurements of α_3 , M_h and M_t will allow to establish if the conditions are satisfied (see e.g. figure 14 of [9] and figure 5 of [11]). A possible anthropic origin of their values would arise if the value of the parameters are close to the anthropic boundary defined by these conditions.

The rest of this paper is organized as follows. In section 2 we review the vacuum stability issue and the perspectives for future progress by improving the determination of the relevant parameters. We will see that the High Luminosity stage of the LHC (HL-LHC) can reduce the uncertainty on M_h down to a sufficient level, while a fully satisfactory determination of α_3 would require a factor 10 improvement of the current lattice precision, or a factor of 3 improvement of the sensitivity of the FCC-ee future collider (when theoretical uncertainties are taken into account) that is the most effective one for this measurement. Finally the measurement of M_t can only be improved by a future lepton collider operating close to the threshold for top quark pair production. The requirement specifications for such collider, in terms of the integrated luminosity and of the beam energy spread that is required for a sufficiently accurate M_t measurement, is studied in section 3. The measurement can be performed at proposed future colliders, such as FCC-ee [12], CLIC [13, 52, 57] and ILC [14], with a much wider scope than the top mass determination. We argue that

unconventional sufficient alternatives for this specific measurement could be an e^+e^- collider in the LHC tunnel (also known as LEP3) or a very compact ‘demonstrator’ stage of a $\mu^+\mu^-$ collider. Finally, we report our conclusions in section 4.

2 The SM vacuum (in)stability

As discussed in the introduction, measurements aimed at establishing the existence of a second minimum in the SM Higgs potential, such that the physical minimum is unstable, are of strategic relevance from the landscape perspective. In this section we summarize the current status and the future perspectives for the assessment of the (in)stability of the SM vacuum.

The Higgs quartic coupling λ extrapolated around the Planck scale. The sign of the Higgs quartic coupling λ extrapolated at the Planck scale M_{Pl} controls the existence of the second minimum. Its current central value is slightly negative, suggesting that the second minimum exists. Using the $\overline{\text{MS}}$ scheme for λ and α_3 and the pole mass definition for M_t and M_h , for values of the parameters close to the current central values, it equals (see also [16])

$$\lambda(M_{\text{Pl}}) \simeq -0.0096 - 0.0065 \left(\frac{M_t}{\text{GeV}} - 172.6 \right) + 0.0024 \frac{\alpha_3(M_Z) - 0.1179}{0.0009} + 0.0030 \left(\frac{M_h}{\text{GeV}} - 125.1 \right). \tag{2.1}$$

The RG running of the quartic coupling is shown in figure 1 (left panel) including variations of M_t , α_3 and M_h within their present $\pm 5\sigma$ ranges. The details of the evolution shown in figure 1 depend on the assumed central value. For M_t we employ a central value close to the average of the LHC results, with an uncertainty corresponding to the latest published results (coming from the 7 TeV and 8 TeV runs)

$$M_t = \begin{cases} 172.69 \pm 0.25_{\text{stat}} \pm 0.41_{\text{syst}} & \text{ATLAS, 20.2/fb [17]} \\ 172.44 \pm 0.13_{\text{stat}} \pm 0.47_{\text{syst}} & \text{CMS, 29.7/fb [18]} \\ 174.30 \pm 0.35_{\text{stat}} \pm 0.54_{\text{syst}} & \text{CDF, D0, } \leq 9.7/\text{fb [19]} \end{cases} \tag{2.2}$$

For α_3 and M_h we pick the current PDG [20] value and their uncertainties.

With the current central values, the Higgs quartic is negative at high energy, but the opposite sign cannot be excluded at the 5σ level. Establishing firmly that the high energy Higgs quartic is negative is thus a clear first target for future investigations in this area. We see in the left panel of figure 1 that the current uncertainty on M_h is sufficient for this task, and only a mild improvement on α_3 is needed. The uncertainty on M_t should instead significantly decrease, reaching $\delta M_t \approx 250$ MeV. It should be emphasized that these estimates are strongly sensitive to the central value assumed by the parameters. For instance if M_t was lower by 1 GeV, half of the measurement precision estimates above would not yet quite be sufficient to establish instability.

A second target is the determination of the scale at which λ crosses zero and runs negative. This scale is largely uncertain, ranging from 10^8 GeV up to the Planck scale with the current 1σ errors of the SM parameters. It should be noted that the scale of crossing

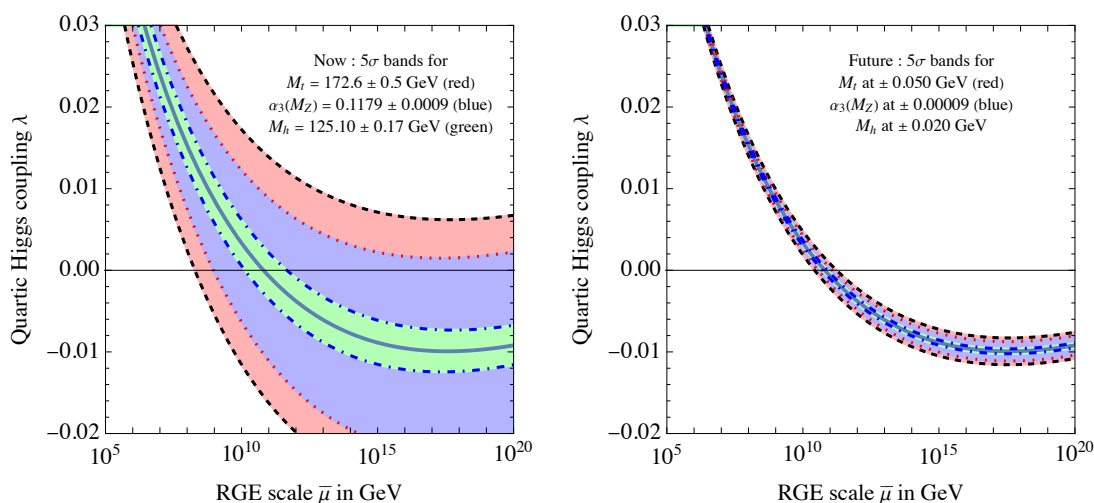


Figure 1. Running of the quartic Higgs coupling, that determines the Higgs potential and its instability scale. The $\pm 5\sigma$ bands associated with the uncertainty in the top quark mass M_t are plotted as dashed gray, those associated to $\alpha_3(M_Z)$ as dotted red, those associated to M_h as dot-dashed blue.

is gauge-dependent and thus unphysical. A physical gauge-independent definition of the scale of instability is provided instead [9, 16] by the maximal height of the Higgs potential barrier, namely $\Lambda^4 = \max_h V_{\text{eff}}(h)$. This is given by [16]

$$\log_{10} \frac{\Lambda}{\text{GeV}} = 10.5 - 1.3 \left(\frac{M_t}{\text{GeV}} - 172.6 \right) + 0.6 \frac{\alpha_3(M_Z) - 0.1179}{0.0009} + 1.1 \left(\frac{M_h}{\text{GeV}} - 125.1 \right), \tag{2.3}$$

where M_t and M_h are the pole top and Higgs masses and the $\overline{\text{MS}}$ scheme is used for α_3 .

In order to assess the necessary precision to ‘measure’ the instability scale we propagate uncertainties in eq. (2.3) and show in figure 2 the resulting relative uncertainty $\delta\Lambda/\Lambda$ that corresponds to a given precision in the measurement of each of the three parameters M_t , M_h , and α_3 . The top mass and α_3 are currently the largest sources of uncertainties, while M_h is almost precise enough to determine the instability scale. Setting an arbitrary threshold of around 20% precision on Λ , figure 2 shows that an absolute error of around 10^{-4} would be needed on α_3 , while the top mass should be known with error $\delta M_t = 50$ MeV.

Improved M_t determination prospects. As the uncertainty on M_t is reflected on the largest uncertainty on eq. (2.3), we start from discussing the prospects for progress in its determination. As we assume the validity of the SM up to very short length scales, the evaluation of the performance of each experiments is evaluated under this assumption. Top quark loops affect various lower-energy observables, that are thereby sensitive to the top quark mass. Previous work found that SM fits will not allow precise enough measurements of the top mass M_t [21]. As a consequence, the only option to measure M_t better is to measure it at future colliders.

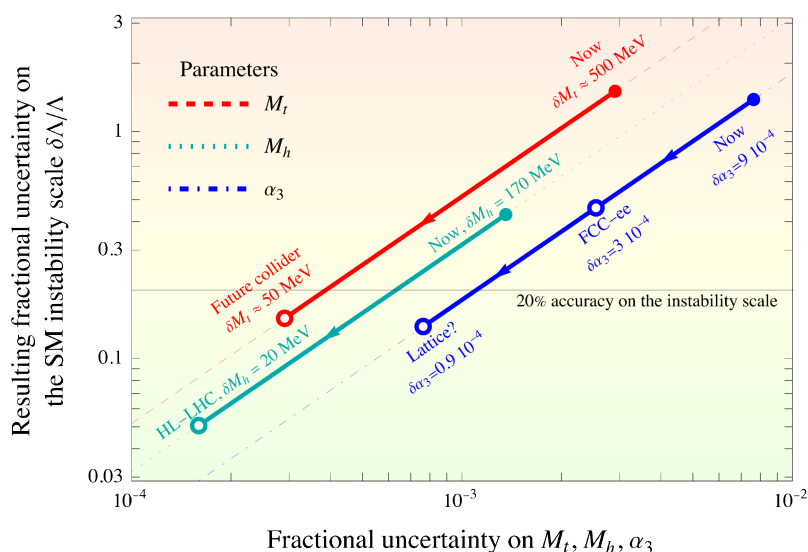


Figure 2. The 1σ relative uncertainty on the scale of instability determined by eq. (2.3) as function of the relative precision of the measurements of α_3 , M_t , and M_h . The horizontal shade at 0.2 corresponds to a determination of the instability scale at 20% precision. The current situation and future improvements are marked as full and empty dots, respectively.

In this context the HL-LHC stands in a delicate position as the top quark sample is already large enough that systematic uncertainties dominates in analysis of the 7+8 TeV LHC data. Indeed, measuring the top quark mass summing the energies of its visible decay products is like measuring the pig mass summing sausages: higher statistics allows a better Monte Carlo modeling, but leaving systematic uncertainties untouched. The present uncertainty about 500 MeV is at the limit to which tools such as leading-log Monte Carlo parton shower generators are considered trustable. The inclusion of higher perturbative orders in the matrix elements attached to the present parton showers can improve this situation, but a measurement of M_t with uncertainty comparable to Λ_{QCD} remains challenging. Thus we consider unlikely that the HL-LHC will improve the present uncertainty on M_t by the substantial factor that is needed to firmly establish the scale of the SM instability.

Also enlarging the scope of HL-LHC to ‘alternative’ strategies for the top quark mass measurements, e.g. reviewed in [22], we find a limited improvement compared with the target imposed by our question. Even barring experimental uncertainties, the ‘alternative’ methods are hitting the limitations of the present computations in describing effects commensurate with Λ_{QCD} either because of matching of fixed order and parton shower computations in the ‘alternative’ observables [23], or uncertainties in the knowledge of hadronization physics [22], or possible lack of understanding of the effects of the colored environment [24] in which the short-distance $t\bar{t}$ are produced at LHC and so on. All in all, we will need a future collider beyond the HL-LHC to measure the top quark mass with sufficient precision to ‘measure’ the instability scale. Great prospects are offered by e^+e^- colliders, and in principle $\mu^+\mu^-$ colliders, that can determine the top quark mass from a center-of-mass energy scan around the threshold of the $\ell^+\ell^- \rightarrow t\bar{t}$ reaction around $2M_t$ [13, 25–27]. This will be discussed in section 3.

Improved α_3 determination prospects. The present knowledge of α_3 results in a subdominant uncertainty on the instability scale compared to M_t . Still it is too large to draw conclusions on the fate of the quartic coupling at high energy. It can in principle be improved pursuing any of the presently employed techniques reviewed in [20].

The most precise present determinations of $\alpha_3(M_Z)$ from experiments, with an uncertainty of order ± 0.0010 , come from low-energy τ -decay and parton distribution functions fits. The determination from LEP has a larger uncertainty ± 0.0030 dominated by the uncertainty on the lepton/hadron ratio measured at the Z pole, $R_\ell = \Gamma(Z \rightarrow \text{hadrons})/\Gamma(Z \rightarrow \mu^+\mu^-)$, affected at loop order by α_3 and measured with 0.12% uncertainty (mildly dominated by statistics).

According to FCC-ee studies [28–31], exploiting 10^5 times more Z bosons than the full LEP data sample, the uncertainty on R_ℓ can be reduced by a factor 20 down to $\pm 0.005\%$, so that the uncertainty on α_3 can too be reduced by a factor 20, down to ± 0.00016 , barring any theory uncertainty [29]. However by applying projected theory uncertainties onto this extraction of α_3 , ref. [29] gives an estimated ± 0.00030 for FCC-ee and ± 0.00070 for ILC. As the ILC is expected to yield a comparable number of Z boson to ‘site filler’ e^+e^- machines (e.g. at FNAL [32, 33]), we can take the ILC result as a ballpark indication for the possible results of such ‘site filler’ project, or of LEP3 [34, 35] if it is run at the Z -pole.

All in all, the high-energy e^+e^- colliders in the most optimistic scenario can improve a factor around 20 compared to the present determinations from the same type of measurement, or, expressed differently, a factor around 5 compared to the present world-average. From the current central value, the FCC-ee determination of α_3 would be sufficient to establish the change of sign of the Higgs quartic at more than 5σ , while ILC or LEP3 would do that at around 5σ . None of these measurements, however, would precisely pinpoint the scale of the instability, as shown in figure 2.

The present most precise single ‘measurement’ of α_3 is obtained from lattice QCD calculations of suitable quantities [36]. Based on the extrapolations of ref. [37] on the reduction of the computing cost, and on their estimates of the impact of adding more perturbative orders, reduction of lattice spacing, and accumulated statistics, an improvement of the current lattice QCD uncertainty on α_3 by a factor up to 10 can be expected in the next decade at fixed computing cost by adding one order in perturbation theory inputs in the lattice extraction of α_3 . More recent estimates on the progress of the lattice QCD determination of α_3 contained in [38] give less optimistic prospects. Such factor 10 improvement would be sufficient, according to figure 2, for a 20% precision on the instability scale determination.

Improved M_h determination prospects. The Higgs boson mass as currently measured at the LHC has a small impact on the instability scale thanks to an already quite precise measurement. Knowledge of M_h can be improved by future HL-LHC measurements in clean channels such as $h \rightarrow 4\ell$ and $h \rightarrow \gamma\gamma$. Exploiting a dataset larger by about two orders of magnitude, the HL-LHC could reach around 20 MeV uncertainty [39]. This is well below the target for 20% measurement of the scale Λ (see figure 2).

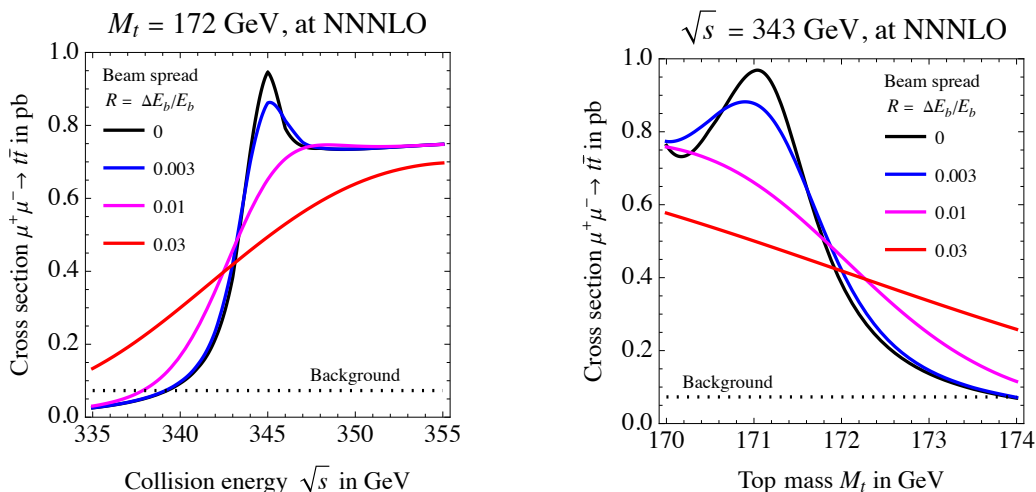


Figure 3. Cross section for $\ell^+\ell^- \rightarrow t\bar{t}$ around threshold at NNNLO accuracy and including Higgs-EW corrections, obtained with the `QQbar_threshold` code [47, 48]. The background estimated for the CLIC analysis in [13], of 73 fb, is reported as a dotted line. *Left:* as function of \sqrt{s} , fixed M_t . *Right:* as function of M_t , fixed \sqrt{s} . We here employ the ‘potential-subtracted’ top mass [49].

3 A top threshold collider

The cross section for $\ell^+\ell^- \rightarrow t\bar{t}$ around the kinematical threshold $\sqrt{s} \sim 2M_t$ is strongly sensitive to the top mass [40–46]. The large variation of σ with \sqrt{s} is shown on the left panel of figure 3 (black curve), based on the NNNLO SM predictions from [47, 48]. The spike is due to the $t\bar{t} 1s$ bound state. Correspondingly, as shown on the right panel of the figure, the cross section at fixed \sqrt{s} depends strongly on M_t .³ Thanks to the high sensitivity to M_t

$$\frac{d \ln \sigma}{d \ln M_t} \sim 1.6 \frac{M_t}{\Gamma_t} \approx 200, \quad (3.1)$$

a cross section measurement with modest 10% relative accuracy enables a determination of the top quark mass at the 0.05% level. The cross section close to the threshold is around 500 fb, therefore a collider integrated luminosity as small as $\mathcal{L} \simeq 0.2 \text{ fb}^{-1}$ is sufficient for a 10% statistical uncertainty on the cross section measurement. In turn, based on the rough estimate above, this measurement could enable a determination of the top mass with $\delta M_t = 5 \cdot 10^{-4} M_t = 86 \text{ MeV}$, close to the instability scale measurement target of $\delta M_t = 50 \text{ MeV}$, figure 2.

The vast literature (see e.g. [13, 50–54]) on $t\bar{t}$ threshold cross section measurements at lepton colliders considers a relatively large integrated luminosity (typically, $\mathcal{L} \sim 100 \text{ fb}^{-1}$), which can be available at colliders like CLIC, ILC, CEPC and FCC-ee, and quantifies the expected error on M_t based on the properties (eminently, the shape in energy of the luminosity spectrum) of the specific collider project under examination. Here instead we want to assess the characteristics that a generic collider should possess, in terms of integrated luminosity and luminosity spectrum, for a sufficiently accurate determination of M_t .

³In the plot, and in the rest of this section, we employ the ‘potential-subtracted’ top mass [49].

Furthermore, existing studies of the top threshold have a broader target than the determination of M_t , including independent measurements of the top quark width Γ_t and of the top Yukawa coupling y_t . From our perspective instead, Γ_t and y_t are predicted by M_t and the other SM parameters, because no new physics exists to modify the SM relations. All these parameters can be independently accurately determined with $\mathcal{L} = 100 \text{ fb}^{-1}$ and a scan on the center of mass energy E_{cm} of the collider at ten points with equal integrated luminosity, spaced by 1 GeV, which is the baseline running scenario for most of these studies. This scan setup is not far from optimal [13] for the simultaneous determination of all these parameters, but expectedly not so (see [13] for a discussion) if the only target is the M_t determination as in our case. A reassessment of the scan strategy is needed.

Apart from the luminosity, the most important feature that a top threshold collider must possess for an accurate M_t determination is a luminosity spectrum that is narrowly localized around the nominal collider energy, $\sqrt{s} \simeq E_{\text{cm}}$. We model the spectrum with a Gaussian centered at E_{cm} and standard deviation $R/\sqrt{2} E_{\text{cm}}$, with $R = \Delta E_b/E_b$ the energy spread of each beam. The relative standard deviation $R/\sqrt{2}$ should be compared with the width of the cross section shape on the left panel of figure 3, which in turn can be estimated as Γ_t/M_t . If it is much smaller than that, namely if $R \ll \Gamma_t/M_t \sim 1\%$, the cross section is not affected by the convolution and the shape of $\sigma(E_{\text{cm}}, M_t)$ displays the strong dependence on E_{cm} and M_t previously described. On the other hand, if R is larger the dependence is smoothed out significantly, as shown by the colored lines in figure 3, entailing a reduction of the M_t measurement precision.

The heuristic considerations above can be summarized in the following estimate for the error

$$\delta M_t \approx \frac{\Gamma_t}{1.6\sqrt{N_t}} \left[1 + \left(\frac{M_t R}{0.5 \Gamma_t} \right)^2 \right]^p, \quad N_t = \mathcal{L} \langle \sigma \rangle, \quad \langle \sigma \rangle \approx 0.5 \text{ pb}, \quad (3.2)$$

where N_t is the total number of produced $t\bar{t}$ events. The scaling with $1/\sqrt{N_t}$ is dictated by the statistical accuracy in the cross section measurement, and the prefactor is chosen according to eq. (3.1). The factor 0.5 arises matching a Breit-Wigner with a Gaussian. The power $p \approx 0.45$ arises in view of the specific shape of $\sigma(E_{\text{cm}}, M_t)$, and mostly depends on how the sensitivity in eq. (3.1) is reduced at large R .

For a solid estimate of the uncertainty we include the smearing due to the energy spread in the cross section predictions and we perform a χ^2 fit to the top mass using measurements at several E_{cm} points. A constant background of 73 fb, from the CLIC analysis in [13], is considered in the analysis. The results are displayed in figure 4 as δM_t contours in the (\mathcal{L}, R) plane. The figure assumes 70% efficiency in the reconstruction of the two top quarks [13]. The effects of Initial State Radiation (ISR) of photons, which are significant for e^+e^- colliders as we will see, are not included in the figure. Only statistical uncertainties are included in the fit. We later comment on the expected systematic and parametric uncertainties.

The left panel of figure 4 shows the results for ten collider E_{cm} points, equally spaced by 1 GeV starting at 340 GeV, with equal luminosity, of $\mathcal{L}/10$, collected at each run. The precision on M_t is significantly inferior than the one estimated by eq. (3.2), and correspondingly a higher luminosity is needed to attain a given δM_t target. For instance $\delta M_t = 50 \text{ MeV}$, for

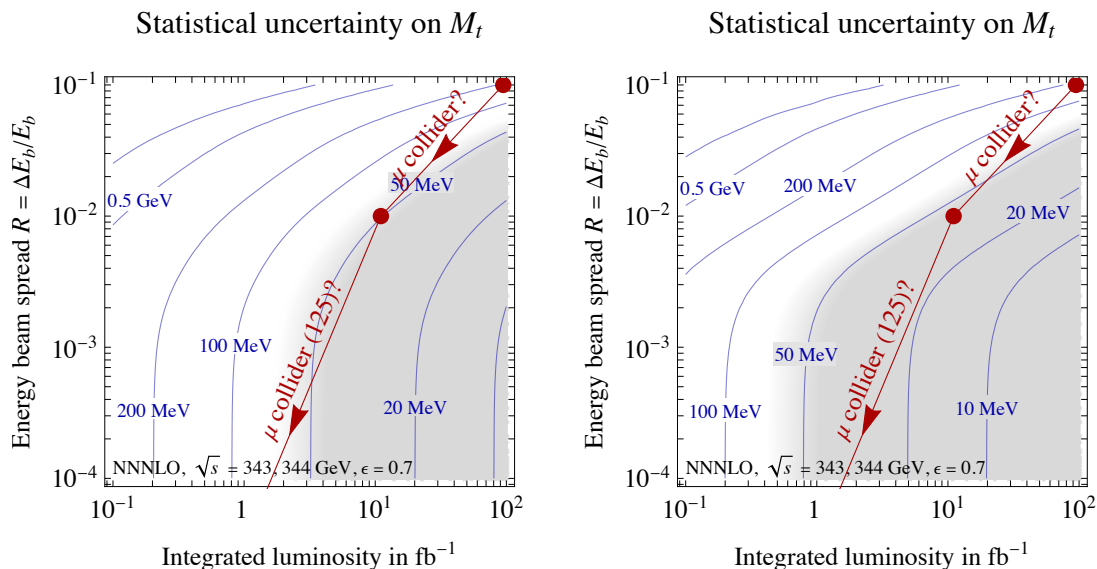


Figure 4. *Statistical uncertainty on the top mass.* Initial State Radiation is neglected, as appropriate for a muon collider. The left panel assumes running at 10 values of $E_{\text{cm}} = \{340, 341, \dots, 349\}$ GeV with $\mathcal{L}/10$ luminosity at each point. The right panel assumes running at $E_{\text{cm}} = \{342, 343\}$ GeV with $\mathcal{L}/2$ luminosity at each point. The results are reported in the plane formed by the beam energy spread R , and the luminosity \mathcal{L} . We assumed a 70% efficiency for $t\bar{t}$ reconstruction. In the shaded region the systematic uncertainty on M_t estimated in eq. (3.3) is larger than the statistical uncertainty.

negligible R , requires more than 3 fb^{-1} , while 0.8 fb^{-1} would suffice according to eq. (3.2) including the 70% efficiency. This is because the threshold scan points are not optimized for the sensitivity to M_t , as previously explained. The best results would be obtained by collecting the entire luminosity at the single point that maximizes the sensitivity. For a true value of $M_t = 172 \text{ GeV}$, which we assume for our analysis, the optimal point would be at $E_{\text{cm}} = 343.5 \text{ GeV}$, nearly independently of the beam energy spread. However with a single energy point the χ^2 often displays a secondary minimum, and furthermore a running scenarios with multiple energy points is arguably favored for the reduction of systematic uncertainties that are correlated at the different points.

We thus consider two energy points spaced by 1 GeV, whose optimal positions are found to be at 333 and at 334 GeV. This configuration improves the result significantly, as shown on the right panel of figure 4. The improvement is less pronounced at large R , because the beam energy spread flattens out the dependence of the cross-section on E_{cm} , asymptotically making all the points in the threshold region equally sensitive to M_t . The right panel of the figure is in good agreement with the estimate in eq. (3.2).

The scan optimization depends on the true value of M_t , especially when R is small, since the optimization is less relevant for large beam energy spread as previously explained. The true top mass is uncertain. Therefore the luminosity estimates on the right panel of the figure should be taken with care, while the ones on the left panel are more robust to the true value of M_t . On the other hand the true value of M_t can be determined with increasing

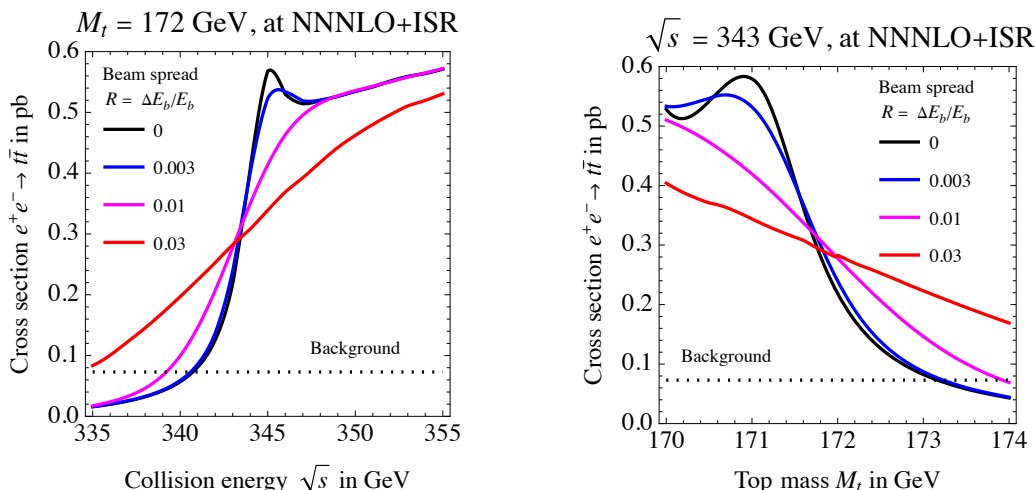


Figure 5. As in figure 3, but with Initial State Radiation included, as appropriate for a e^+e^- collider.

accuracy during the collider operation, enabling an improved determination of the optimal points. Some tests we performed assuming the top mass in a safe confidence range, chosen on the basis of the present-day error, suggest that around twice the luminosity estimated with two optimized scanning points are sufficient to match the accuracy. For instance, 2 fb^{-1} is enough for $\delta M_t = 50 \text{ MeV}$ at small R . For larger $R \gtrsim 10^{-2}$, $\delta M_t = 50 \text{ MeV}$ requires more luminosity, but still below 10 fb^{-1} .

Initial state radiation. The estimates presented so far apply to a muon collider, while for e^+e^- colliders the low mass of the electron entails a significant impact of photons ISR on the cross section, shown in figure 5. The effect of ISR is doubly negative. It lowers the value of the cross section close to the threshold and it reduced its sensitivity to the top mass. The result, shown in figure 6, is an increase of the required luminosity of a factor almost 3 at small R . The increase is less prominent when the beam energy spread is larger, so that ISR has a relatively milder impact on the collision energy spectrum.

Our results for 10 energy points, including ISR, are in good agreement with the literature. For instance, the FCC-ee collider with $\mathcal{L} = 200 \text{ fb}^{-1}$ and beam energy spread $R = 2 \cdot 10^{-3}$ [20] could measure M_t (when Γ_t is varied with M_t according to the SM relation) with $\pm 9 \text{ MeV}$ statistical uncertainty [54]. CLIC could reach $\pm 21 \text{ MeV}$ [52] with the half luminosity and energy spread $R = 2 \cdot 10^{-3}$ [55]. The CLIC performances are slightly inferior, and in less good agreement with our estimate, possibly because of the beam-beam interaction effects, typical of linear colliders, that slightly reduce the luminosity in the threshold region.

Systematic and parametric uncertainties. Several sources of uncertainty should be included for a realistic analysis, in addition to the statistical uncertainty we have estimated. First, one should consider experimental systematic uncertainties in the measurement of the cross section due to the uncertainties on the determination of the luminosity and of the $t\bar{t}$ acceptance and reconstruction efficiency, or on the background estimate. These uncertainties should be compared with the statistical uncertainty on the cross section measurements,

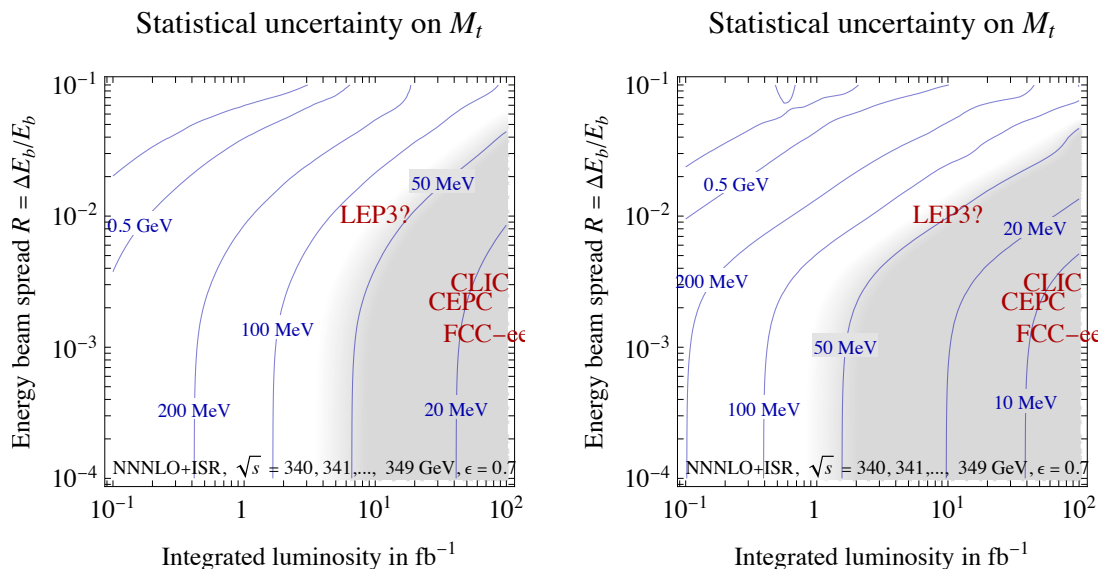


Figure 6. As in figure 6, with Initial State Radiation effects included, as appropriate for a e^-e^+ collider.

which is modest (above one percent) for $\mathcal{L} \lesssim 10 \text{ fb}^{-1}$. Experimental systematics are thus expected to play a minor role.

Uncertainties also emerge from the imperfect knowledge of the beam energy distribution, namely of the central value E_{cm} and of the relative spread R of the distribution. The central value is the reference scale for the measurement, therefore it should be known better than $\delta M_t/M_t$ (0.03%, for $\delta M_t = 50 \text{ MeV}$) not to impact our findings. The uncertainty on R has no effect when R is negligible but it can impact our results significantly when R is of order few per mille or larger and the cross section is affected at order one by the convolution with the beam spectrum. An R determination as accurate as $\delta M_t/M_t$ is expectedly needed in the large R regime. This aspect was investigated in details for linear colliders in [56] (see also [57]), showing that the beam energy distribution parameters can be measured in Bhabha events with enough precision not to affect the top mass determination. The conclusion might hardly be different for circular e^+e^- colliders, but the point should probably be reassessed in the case of muon colliders.

The effect of systematic and parametric uncertainties on the cross section prediction is extensively studied in the literature [13, 50, 52, 58]. They emerge from theory uncertainties on the resummation of threshold corrections, as well as from fixed order scale variations which alone amount to around 40 MeV [50]. Current uncertainties from α_3 are expected to become negligible with the improvement on the α_3 determination envisaged in the previous section. We thus expect systematic uncertainty on M_t of around

$$\delta M_t|_{\text{syst}} \approx 40 \text{ MeV}. \quad (3.3)$$

A total uncertainty $\delta M_t = 50 \text{ MeV}$, that is expected to settle the vacuum stability question conclusively as discussed in section 2, should thus be feasible. The results of the present section show that a top threshold collider with moderate beam energy spread could

Collider		LEP	LEP3	FCC-ee [31]	CEPC [59]
Total length L		26.6 km	26.6 km	100 km	100 km
Z	$E_{\text{cm}} = 91 \text{ GeV}$	~ 0.004	7^*	460	115
W^+W^-	$E_{\text{cm}} = 160 \text{ GeV}$	~ 0.01	2^*	56	16
Zh	$E_{\text{cm}} = 240 \text{ GeV}$	0	1 [35]	17	5
$t\bar{t}$	$E_{\text{cm}} = 350 \text{ GeV}$	0	0.1^*	3.8	0.5

Table 1. Expected luminosities in $10^{34} \text{ cm}^{-2}\text{s}^{-1}$. The * stands for our estimate, based on rescalings from available literature.

attain comparable statistical precision with few/fb integrated luminosity. This is a factor of 20 less luminosity than the one foreseen at the currently proposed top threshold colliders.⁴

Unconventional top threshold colliders. The ILC, CLIC and FCC-ee are mature well-studied collider projects that can match (and overcome) the $\delta M_t = 50 \text{ MeV}$ statistical precision target as previously discussed. We devote the rest of this section to speculate on the feasibility of the top mass measurement at unconventional colliders that might (or not) be convenient to build given financial or strategic considerations. Specifically, we consider an extension of the ‘LEP3’ e^-e^+ proposed future collider, and a muon collider.

LEP3 [34, 35] is a possible circular e^-e^+ circular collider in the existing LHC tunnel (previously used for LEP) with length $L = 26.6 \text{ km}$. Multiple advances in accelerator physics enable to reach 240 GeV with $10^{34} \text{ cm}^{-2}\text{s}^{-1}$ instantaneous luminosity, as in table 1, to measure the Higgs couplings precisely. The possibility of operating LEP3 at the top threshold $E_{\text{cm}} \simeq 350 \text{ GeV}$ has not been studied, and is challenging for multiple reasons. Rough estimates of the conceivably achievable luminosity, merely based on the power emitted by synchrotron radiation, can be obtained as follows:

- Rescaling LEP3 at $E_{\text{cm}} = 240 \text{ GeV}$. The power emitted by N circulating e^\pm in a ring or radius $r = L/2\pi$ is

$$W_{\text{irr}} = Ne^2(E_{\text{cm}}/2)^4/3\pi r^2 m_e^4. \tag{3.4}$$

This should be smaller than about 100 MW, limiting to $\mathcal{L}_{Zh} \simeq 10^{34} \text{ cm}^{-2}\text{s}^{-1}$ [34, 35, 61] the LEP3 luminosity at $E_{\text{cm}} = 240 \text{ GeV}$. The luminosity scales as $\mathcal{L} \propto E_{\text{cm}} N^2$, where the factor of E_{cm} accounts for the relativistic shrinking of bunches. Therefore with the same radiated power we estimate

$$\mathcal{L}_{t\bar{t}}^{\text{LEP3}} \approx \mathcal{L}_{Zh}^{\text{LEP3}}(240/350)^7 \approx 0.88 \cdot 10^{33} \text{ cm}^{-2}\text{s}^{-1}, \tag{3.5}$$

for the LEP3 collider at the top threshold $E_{\text{cm}} = 350 \text{ GeV}$.

- Rescaling FCC-ee/CEPC at $E_{\text{cm}} = 240 \text{ GeV}$. The planned FCC-ee and CEPC circular collider with a length $L = 100 \text{ km}$ produce $\mathcal{L}_{\text{FCC-ee}} \approx 4 \cdot 10^{34} \text{ cm}^{-2}\text{s}^{-1}$ [54] and $\mathcal{L}_{\text{CEPC}} \approx 0.5 \cdot 10^{34} \text{ cm}^{-2}\text{s}^{-1}$ [59, 60] instantaneous luminosity at $E_{\text{cm}} = 350 \text{ GeV}$. The

⁴These colliders have broader scope than the measurement of M_t , which justifies the higher target luminosity.

luminosity scales as $\mathcal{L} \propto N^2/L$ with the collider circumference, owing to the reduction of the collision frequency with L . Assuming again that the limiting factor is the total radiated power of eq. (3.4) we thus find that the luminosity achievable in the smaller existing LEP tunnel is

$$\mathcal{L}_{t\bar{t}}^{\text{LEP3}} \approx \mathcal{L}_{t\bar{t}}^{\text{FCC-ee}}/3.76^3 \approx 0.75 \cdot 10^{33} \text{cm}^{-2} \text{s}^{-1}, \quad (3.6)$$

in good agreement with the previous estimate. Obviously a factor 8 less luminosity would be obtained by rescaling CEPC.

- A similar estimate, $\mathcal{L}_{t\bar{t}}^{\text{LEP3}} \approx 2 \cdot 10^{33} \text{cm}^{-2} \text{s}^{-1}$ is obtained rescaling in both radius and energy the claim $\mathcal{L}_{Zh}^{16 \text{ km}} \approx 5.2 \cdot 10^{33} \text{cm}^{-2} \text{s}^{-1}$, for a 100 MW collider with $L = 16 \text{ km}$ [62].

As we rescaled collider claims optimized for different lengths and energies, possible adaptations of the collider parameters (number of bunches, β , emittance) could lead to a mildly higher luminosity. For example the luminosity scales with a milder $1/E^{1.8}$ up to when beamstrahlung effects become relevant [63, 64].

A significant challenge for the LEP3 collider operating at the $t\bar{t}$ threshold is the large beam energy loss of 28 GeV per turn, $(175/104.4)^4 \approx 8$ times higher than at LEP with $E_{\text{cm}} = 104.4 \text{ GeV}$. This needs to be compensated by accelerating cavities dE/dx in a few % fraction of the ring circumference. LEP used energy gradient $dE/dx = 7 \text{ MeV/m}$, but $dE/dx = 45 \text{ MeV/m}$ is now possible [65]. Even if the total energy loss in one turn could be compensated, it would still be challenging to maintain the beam in a stable orbit while the energy is emitted. If all these challenges could be successfully addressed, a luminosity of order $\mathcal{L} = 10^{33} \text{cm}^{-2} \text{s}^{-1}$ could be realistic as previously estimated. This corresponds to an integrated luminosity $\mathcal{L} = 10 \text{ fb}^{-1}$ for one year run.

We are obviously not in the position to estimate the beam energy spread that could be possibly attained, that depends in a non-trivial way on the energy and on the machine optics, and on the deployment of appropriate monochromatization techniques that allow a trade between the energy spread and luminosity. Based on our results in figure 6, a percent-level beam energy spread (ten times worse than LEP, where $R \approx 10^{-3}$) would be needed to attain the $\delta M_t = 50 \text{ MeV}$ target if $\mathcal{L} = 10 \text{ fb}^{-1}$.

We finally briefly comment on the possibility of a $\mu^+ \mu^-$ top threshold collider. This option could be considered as a possible ‘demonstrator’ stage of a future very high energy muon collider of $E_{\text{cm}} = 10 \text{ TeV}$ or more [66], that is currently being investigated by the International Muon Collider Collaboration (IMCC) [67]. Such ‘First Muon Collider’ was actually proposed long ago [68].⁵

The potential performances of a top threshold muon collider in terms of luminosity and beam energy spread are difficult to estimate. Two parameter sets are proposed in [69]. The first one is equivalent to our guessed LEP3 performances, with energy spread $R = 10^{-2}$

⁵The uncertainty estimated in [68] for 100 fb^{-1} is in good agreement with ours, taking into account that a $t\bar{t}$ efficiency $\epsilon = (0.3)^2$ (much lower than the realistic $\epsilon = 0.7$ [13] we employ) is assumed in [68]. Furthermore, the NNNLO cross-sections we employ give better sensitivity than the ones at NLO used in [68].

and $\mathcal{L}_{\text{MuC}} = 10^{33} \text{cm}^{-2} \text{s}^{-1}$, and it is sufficient for the $\delta M_t = 50 \text{MeV}$ target for one year run. The total length L of this collider would be $L = 700 \text{m}$. Notice that the sensitivity of muon colliders (in figure 4) is slightly better than the one of e^+e^- colliders because of the absence of ISR.

The second parameter set of [69] foresees instead a ten times larger luminosity, accompanied by a ten times larger energy spread. This configuration is disfavored for the measurement of M_t , but it gives the idea of the large variability of the estimates and of the possibility of raising the luminosity at the cost of increasing the energy spread. The opposite is also possible, as shown by the parameters proposed for a Higgs-pole muon collider at 125 GeV [66, 70]. In this case, the energy spread is 250 times smaller than in the first estimate, $R = 4 \cdot 10^{-5}$, and the luminosity is only 10 times smaller. For the measurement of M_t a much larger $R = 10^{-3}$ is perfectly adequate, and more effective than $R = 10^{-2}$. It would be interesting to optimise the luminosity of the top threshold muon collider at this value of R . These options are visualized as dots connected by lines in figure 4.

4 Conclusions

The lack of new physics that keeps the weak scale and the vacuum energy naturally small suggests anthropic selection in a landscape of vacua, and thereby the possibility that no new physics exists within the reach of next colliders. We provided a first assessment of the potential of future colliders under this assumption. In this situation, all what experiments can (and must) do is to measure the fundamental input parameters of the SM with increasing accuracy. If the SM is part of a landscape of vacua, accurate measurements will generically help to test if it is part of a landscape, and locate it. While the concrete deployment of this program requires information on the detailed structure of the landscape theory that we do not currently possess, we argued that strategic measurements are those needed to assess the existence of a second minimum in the Higgs potential for Planck-scale values of the Higgs vacuum expectation value, namely the determinations of M_t , α_3 and M_h .

In section 2 we defined accuracy targets for the measurement of these quantities, based on two distinct criteria. The first criterion, more loose, is that we would like to establish with 5σ ‘certitude’ that the second minimum exists, as suggested by the current central values. The second criterion, more ambitious, is the request to be able to perform a measurement of the scale of SM vacuum instability (defined, for example, as the maximal height of the potential barrier) with some reasonable accuracy, say 20%.

The most ambitious accuracy target for the measurement of M_h can be attained at the HL-LHC. The target accuracy for α_3 is a factor of 3 lower than what the most precise future collider project (FCC-ee) could achieve, and it is a factor 10 lower than the current lattice QCD determination. Such improvement from the lattice has been claimed to be possible in the literature, but also the opposite has been claimed.

The situation for M_t is more clear. The target uncertainty $\delta M_t = 50 \text{MeV}$ can be definitely (and only) obtained building a lepton collider operating at the top threshold. Several well-established future colliders such as FCC-ee, CLIC, CEPC and ILC can attain this target. They can actually achieve a smaller statistical error on M_t , which however hits system-

atic uncertainties that can be hardly reduced below 40 MeV. This singles out $\delta M_t = 50$ MeV as the target for top mass determination regardless of vacuum instability considerations.

In section 3 we revisited the top mass determination from $\ell^+\ell^- \rightarrow t\bar{t}$ cross section measurement close to the top threshold, with the aim of identifying the minimal specification requirements for a lepton collider to measure M_t with error $\delta M_t = 50$ MeV. We pointed out that the integrated luminosity $\mathcal{L} \approx 100 \text{ fb}^{-1}$ that is generically assumed for the threshold scan is unnecessary for $\delta M_t = 50$ MeV precision. A luminosity of few fb^{-1} is sufficient if the purpose, like in our case, is to measure only the fundamental SM parameter (i.e., the top Yukawa coupling) associated with M_t . A larger luminosity might be needed for an independent determination of other parameters like Γ_t , which is relevant only as a probe of new physics, which however we assumed not to exist.

Our results might offer a guidance to the design of ‘unconventional’ top threshold colliders to be built in place or in addition to the top-threshold stage of the other projects, if strategically convenient. One parameter that controls the quality of the beam for the measurement of M_t is the beam energy spread R , whose optimal value is around 10^{-3} or below. The other parameter is the nature of the beam. In particular muon beams are favored over electrons because Infrared State Radiation effects reduce the sensitivity. We briefly discussed the possibility of upgrading the LEP3 e^+e^- collider up to the top threshold, and of building a compact $\mu^+\mu^-$ dedicated collider. This latter option could be considered as a possible ‘demonstrator’ stage of a future very high energy muon collider. Dedicated studies are needed.

A Increasing the information content of known physics

More precise measurements of the SM parameters allow us to locate more precisely the SM in the landscape of vacua, i.e. to gain information on the specific vacuum ‘ v ’ realized in our universe. Notions from information theory can thus be employed to quantify the information gain. An attempt in this direction is presented in this appendix.

A.1 General information-theory discussion

In order to proceed, we label vacua by an integer $v = \{1, \dots, N\}$, and interpret it as instances of a statistical variable ‘ V ’. In the most uncertain situation, we could be in each vacuum v with probability equal probability $\wp(v) = 1/N$. Therefore the Shannon entropy of the variable V that describes the landscape is

$$H(V) = - \sum_{v=1}^N \wp(v) \ln \wp(v) = \ln N. \tag{A.1}$$

The Shannon entropy tells the number of information digits in the basis of the Euler number (e -digits) that must be measured in order to identify the vacuum uniquely among the N options. For instance if $N = 10^{500} \simeq e^{1200}$, the number of required e -digits equals $\ln N \simeq 1200$. When adding information by means of measurements, only the vacua similar to the SM remain compatible with available information and less digits of information will be needed.

We gain information by measuring the n fundamental parameters that characterize the effective QFT for the light particles of each vacuum: the gauge, Yukawa and quartic couplings, and dimensional parameters. We collectively denote them as Y_i with $i = \{1, \dots, n\}$. The value of the parameters is predicted to be $y_{v,i}$ in each specific vacuum v . Assuming (for simplicity) uncorrelated Gaussian distributed measurements with standard deviations σ_i , the probability of the measurements giving as outcome the central values y_i (namely to observe $Y_i = y_i \pm \sigma_i$) assuming vacuum v is

$$\wp(y|v) = \prod_{i=1}^n \frac{1}{\sigma_i \sqrt{2\pi}} \exp \left[-\frac{1}{2} \frac{(y_i - y_{v,i})^2}{\sigma_i^2} \right]. \quad (\text{A.2})$$

Using the (lack of) prior information about which vacuum is physical (i.e., $\wp(v) = 1/N$)

$$\wp(y) = \sum_v \wp(y|v) \wp(v) = \sum_v \frac{1}{N} \wp(y|v). \quad (\text{A.3})$$

After the measurements, the probability of each vacuum v is obtained by the Bayes theorem

$$\wp(v|y) = \frac{\wp(y|v) \wp(v)}{\wp(y)} = \frac{\wp(y|v)}{\sum_w \wp(y|w)}. \quad (\text{A.4})$$

The Shannon entropy for the landscape variable V after the measurements thus becomes

$$H(V|Y=y) = - \sum_{v=1}^N \wp(v|y) \ln \wp(v|y), \quad (\text{A.5})$$

smaller than the value it had before the measurements, $H(V) = \ln N$. Accurate enough measurements are needed in order for the entropy to decrease significantly. This can be seen by noticing that in the limit $\sigma_i \rightarrow \infty$ of very inaccurate measurements the posterior probability $\wp(v|y)$ in eq. (A.4) approaches the flat prior probability $\wp(v) = 1/N$, because $\wp(y|v)$ is independent of v . More specifically, $\wp(v|y)$ can depart from the flat distribution significantly, such that the entropy decreases, only if σ_i is smaller than the interval span by the parameter predictions $y_{v,i}$ across the vacua. Namely, the measurement should be precise enough to discriminate among the vacua.

Eventually the distribution becomes localized on some vacuum \bar{v} , $\wp(\bar{v}|y) = 1$, as σ_i decreases further and becomes much smaller than the minimal separation between the $y_{v,i}$ predictions at different vacua. Such precise measurements identify the vacuum uniquely reducing the entropy to zero, $H(V|Y=y) = 0$, meaning that no additional information is required.

The entropy in eq. (A.5) depends on the values y_i of the parameters that have actually been measured. Generically the entropy is smaller, for given measurement errors, if the measured values y fall in a region that is less densely populated by the landscape. Indeed in that case the minimal separation between the different predictions is larger, and thus it is easier to identify the vacuum. Measurements of parameter values that are atypical in the landscape strategically provide more information. A well known limiting case, dubbed ‘swampland’, arises if the landscape leaves empty regions of parameter space. Observation of parameters in an empty region would falsify the theory that generates the landscape.

However we do not know the parameter density in the vacuum, therefore we cannot exploit the knowledge of the measured values y_i . We can nevertheless proceed as follows. If the landscape theory is correct the measured parameter values will more likely be the ‘typical’ ones predicted by the landscape statistics. Therefore it makes sense to average eq. (A.5) over y_i , obtaining what is known as *conditional entropy* in information theory

$$H(V|Y) = - \int d^n y \sum_{v=1}^N \wp(y) \wp(v|y) \ln \wp(v|y) = - \int d^n y \sum_{v=1}^N \frac{1}{N} \wp(y|v) \ln \wp(v|y). \quad (\text{A.6})$$

The expected average *information gained* by a generic measurement (without knowing its outcome) is then

$$\Delta H = H(V) - H(V|Y) = \int d^n y \sum_{v=1}^N \frac{1}{N} \wp(y|v) \ln \frac{\wp(y|v)}{\wp(y)}. \quad (\text{A.7})$$

The dependence on the measurement uncertainties of the conditional entropy, and in turn of ΔH , is qualitatively the same of the posterior Shannon entropy in eq. (A.5). Namely, there is no information gain (i.e., $\Delta H = 0$) if the measurement uncertainties σ_i are much larger than the range of variability of the parameters in the landscape. The vacuum is fully determined (i.e., $\Delta H = H(V) = \ln N$) if σ_i is much smaller than the typical spacing among the parameter predictions in the different vacua. The information gain increases as the measurement accuracy improves, when σ_i is in the intermediate regime.

This quantitative estimate of ΔH depends on the distribution in the landscape of the parameter predictions. Since this is unknown, no trustable estimate can be performed. However we can illustrate the dependence on the distribution, and obtain tentative results, by considering two specific limiting cases.

First, we assume a generic dense feature-less distribution probability. As a concrete example (results will not depend on the specific assumptions), we assume that the y_i parameters predictions are uniformly distributed in intervals $y_i \in [\mu_i - 1/2, \mu_i + 1/2]$, namely that the $y_{i,v}$ predictions are equally spaced on a square lattice with lattice spacing $a = 1/N^{1/n}$, around central values μ_i . The critical uncertainty below which single vacua can be resolved, such that the entropy vanishes and $\Delta H = \ln N$, is $\sigma_i^c = a$. Uncertainties larger than the length of the y_i intervals do not entail information gain and $\Delta H = 0$. In the intermediate region $\sigma_i^c \ll \sigma_i \ll 1$, $\wp(y)$ in eq. (A.3) is the sum of many Gaussians with the same height, with uniformly spaced centers and a width that is much larger than the separation between the centers. Therefore it approaches the uniform distribution $\wp(y) \simeq 1$ and the information gain can be approximated as

$$\Delta H \simeq \sum_{v=1}^N \frac{1}{N} \int d^n y \wp(y|v) \ln \wp(y|v) = - \sum_{i=1}^n \ln(\sqrt{2\pi e} \sigma_i). \quad (\text{A.8})$$

The validity eq. (A.8) is verified in figure 7 in the toy example of a landscape where $N = 1000$ and $n = 1$: we see that in the intermediate region, where information partially reduces the entropy, the generic formula of eq. (A.8) reproduces the result of eq. (A.7) that takes into account the detailed structure of the landscape.

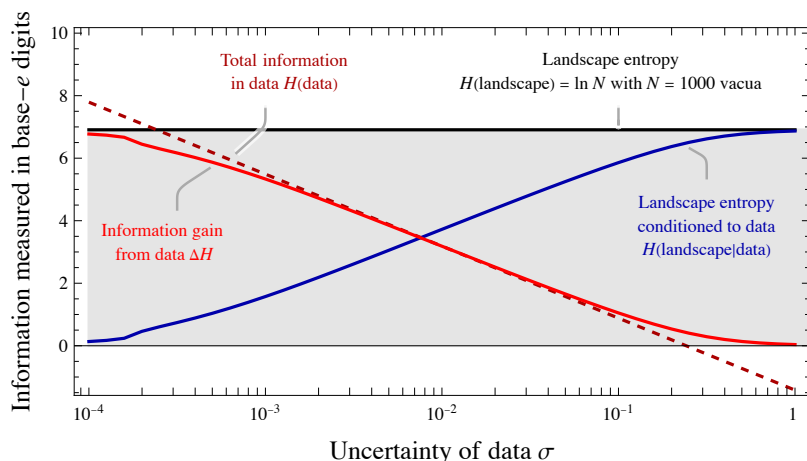


Figure 7. We consider a toy landscape with $N = 1000$ vacua, so that the black horizontal curve at $H(\text{landscape}) = \ln 1000$ shows the Shannon landscape information entropy. This progressively decreases down to $H(\text{landscape}|\text{data})$ as fundamental parameters are measured with smaller uncertainty σ (blue curve). The information gain $\Delta H = H(\text{landscape}) - H(\text{landscape}|\text{data})$ from data (red curve) agrees with the landscape-independent amount of information in data $H(\text{data})$ (dashed red curve) in the intermediate region where the landscape is only partially resolved.

Let us elaborate how the result depends on the unknown landscape distribution for y . For instance if each y_i was still uniformly distributed, but in an interval of length $\Delta y \neq 1$, in eq. (A.8) we would have to rescale $\sigma_i \rightarrow \sigma_i/\Delta y$, finding a finite correction to the universal log-enhanced term.

A less trivial case is when the parameters are logarithmically distributed, namely when the logarithm of the predictions $\ln(y_{i,v})$ are equally spaced in $[\ln(\mu_i) - 1/2, \ln(\mu_i) + 1/2]$ intervals. This situation likely has physical relevance, as the Yukawa couplings and the mass scales in the SM have small numerical values, possibly because of unknown physical mechanisms that naturally give small values, i.e. roughly logarithmic distributions. In this case the landscape probability density is $\varphi(y) \simeq \prod_i 1/y_i$, in the intermediated regime for the measurement uncertainties, eq. (A.7) becomes

$$\Delta H \simeq \sum_{v=1}^N \frac{1}{N} \int d^m y \varphi(y|v) \sum_{i=1}^n \ln[y_i \varphi(y|v)] \simeq - \sum_{i=1}^n \ln(\sqrt{2\pi e} \sigma_i / \mu_i). \quad (\text{A.9})$$

The second equality only holds for measurements with good relative accuracy $\sigma_i/\mu_i \ll 1$.

A.2 Practical physical discussion

This above information-theory expressions just quantify common-sense. For example, let us apply eq. (A.8) to the top Yukawa coupling renormalized at the weak scale. Naively, one would tell that the measurement $y_t = 0.94 \pm 0.03$ provides about one or two digits of information in base 10. The Shannon ΔH tells that y_t contains 2.1 digits of information in base e . So $\Delta H/\ln 10$ is the number of digits in base 10, and $\Delta H/\ln 2$ is the number of bits.

Let us next consider a fundamental physical parameter with small values, such as the muon Yukawa coupling, $y_\mu \approx 0.00060687$. Including the zeros, it provides about 8 digits of information, in agreement with eq. (A.8). Without including the zeros, it only

Symbol	Model description	Number of parameters	Measured bits in base- e	
			including 0	without 0
$g_{1,2,3}$	SM gauge couplings	3	37	36
λ_H	SM Higgs quartic	1	6	6
y_q	SM diagonal Yukawas of quarks	6	50	12
y_ℓ	SM diagonal Yukawas of leptons	3	72	47
V_{CKM}	SM off-diagonal Yukawas of quarks	4	21	11
m_ν	Mass matrix of neutrinos	5	46	9
$v^2/M_{\text{Pl}}^2, V/M_{\text{Pl}}^4$	SM/ Λ CDM mass scales	2	371	10
$\Omega_{m,b,r}, A_s, n_s$	Λ CDM cosmological parameters	5	51	19
All physics		29	655	150

Table 2. The free fundamental parameters of the Standard Model of particle physics and of cosmology, that act as ‘coordinates’ in the landscape, and the number of digits to which they have been measured so far. Some digits get lost, due to QCD uncertainties, when renormalized to higher energy. For a parameter measured as $\mu \pm \sigma$, the column ‘digits including 0’ gives $-\ln \sqrt{2\pi e\sigma}$, as in eq. (A.8). The column ‘digits without 0’ gives $-\ln \sqrt{2\pi e\sigma}/\mu$, as in eq. (A.9). One or the other can be relevant, depending on how small numbers arise in the landscape. We have not included the bound on θ_{QCD} , as the possible existence on axion would allow to relax it.

provides about 5 digits of information, in agreement with eq. (A.9). Indeed the zeros do not provide information that efficiently allows to locate the SM in the landscape if the landscape contains mechanisms that produce small values with high probability (such as a flavour symmetry for the small muon Yukawa coupling, or supersymmetry for the small squared Higgs mass in Planck units).

In addition to experimental uncertainties, computing fundamental parameters $y_{i,v}$ from landscape vacua will have theoretical uncertainties, that should too be included in σ_i . Let us discuss this issue in the context of string theory. String theory seems to need supersymmetry. So far only some supersymmetric string vacua have been computed, and only partially, finding $N = 0$ vacua compatible with the SM, and that many features of low-energy physics are left undetermined, as supersymmetry leaves flat directions in field space. The experimental observation that Nature did not use supersymmetry to keep the Higgs mass fully natural suggests, in the string landscape context, the existence of a huge number of vacua with supersymmetry broken at the string scale. String-theory computations have not yet clarified this issue [15]. Non-supersymmetric vacua are presently uncomputable: we cannot even compute if they exist. If they exist, such vacua can in principle predict values of fundamental constants, as the lack of supersymmetric cancellations allows dynamics to generate minima rather than flat direction.

Presumably, such computations will have theoretical uncertainties such as missing higher-order terms. Presumably, this could mean that theory will not match the high experimental accuracy in parameters such as y_μ . For sure, QCD theoretical uncertainties make part of the measured information unavailable already for the translation of the measurements into determination of the SM parameters: for example $\alpha_{\text{em}}(M_Z)$ is much less accurately known than its low-energy value.

We proceed ignoring theoretical uncertainties on the landscape predictions and quantify the amount of information provided by measurements performed so far. The result is shown in table 2. If ‘0’ count as information, we so far measured about 655 e -bits of information, reducing the landscape entropy by the same amount. If instead small parameters are not rare in the landscape, such that ‘0’ do not have discriminatory power, the amount of measured information is about 160 e -bits.

This amount of measured information should be compared with the unknown amount of diversity in the landscape. For example locating the SM in a landscape of $10^{500} \approx e^{1150}$ vacua roughly uniformly distributed would need measuring $\Delta H \sim 1150$ e -bits. The landscape might have some special structure, making information related to it more relevant. This is why in the next section we focus on measuring strategic parameters that tell if the SM has a deeper vacuum around the Planck scale.

Acknowledgments

We thanks Franco Cervelli, Maurizio Pierini, Philipp Roloff, Alessandro Variola, Marcel Vos, Marco Zanetti, Filip Zarnacki for useful discussions. This work was supported by Italian MIUR under PRIN 2017FMJFMW.

Open Access. This article is distributed under the terms of the Creative Commons Attribution License ([CC-BY 4.0](https://creativecommons.org/licenses/by/4.0/)), which permits any use, distribution and reproduction in any medium, provided the original author(s) and source are credited. SCOAP³ supports the goals of the International Year of Basic Sciences for Sustainable Development.

References

- [1] S. Weinberg, *Anthropic bound on the cosmological constant*, *Phys. Rev. Lett.* **59** (1987) 2607 [[INSPIRE](#)].
- [2] V. Agrawal, S.M. Barr, J.F. Donoghue and D. Seckel, *Viable range of the mass scale of the standard model*, *Phys. Rev. D* **57** (1998) 5480 [[hep-ph/9707380](#)] [[INSPIRE](#)].
- [3] J. Polchinski, *The cosmological constant and the string landscape*, in *23rd Solvay conference in physics: the quantum structure of space and time*, (2006), p. 216 [[hep-th/0603249](#)] [[INSPIRE](#)].
- [4] L. Susskind, *The anthropic landscape of string theory*, [hep-th/0302219](#) [[INSPIRE](#)].
- [5] G. D’Amico, A. Strumia, A. Urbano and W. Xue, *Direct anthropic bound on the weak scale from supernovae explosions*, *Phys. Rev. D* **100** (2019) 083013 [[arXiv:1906.00986](#)] [[INSPIRE](#)].
- [6] N. Arkani-Hamed, S. Dimopoulos and S. Kachru, *Predictive landscapes and new physics at a TeV*, [hep-th/0501082](#) [[INSPIRE](#)].
- [7] P. Ghorbani, A. Strumia and D. Teresi, *A landscape for the cosmological constant and the Higgs mass*, *JHEP* **01** (2020) 054 [[arXiv:1911.01441](#)] [[INSPIRE](#)].
- [8] C.S. Konig et al., *Kelvin, thermodynamics and the natural world*, WIT Press (2016).
- [9] J.R. Espinosa et al., *The cosmological Higgstory of the vacuum instability*, *JHEP* **09** (2015) 174 [[arXiv:1505.04825](#)] [[INSPIRE](#)].

- [10] J. Elias-Miro, J.R. Espinosa, G.F. Giudice, G. Isidori, A. Riotto and A. Strumia, *Higgs mass implications on the stability of the electroweak vacuum*, *Phys. Lett. B* **709** (2012) 222 [[arXiv:1112.3022](#)] [[INSPIRE](#)].
- [11] A. Joti et al., *(Higgs) vacuum decay during inflation*, *JHEP* **07** (2017) 058 [[arXiv:1706.00792](#)] [[INSPIRE](#)].
- [12] A. Maier, *Top pair production and mass determination*, *CERN Yellow Rep. Monogr.* **3** (2020) 117.
- [13] K. Nowak and A.F. Zarnecki, *Optimising top-quark threshold scan at CLIC using genetic algorithm*, *JHEP* **07** (2021) 070 [[arXiv:2103.00522](#)] [[INSPIRE](#)].
- [14] T. Horiguchi et al., *Study of top quark pair production near threshold at the ILC*, [arXiv:1310.0563](#) [[INSPIRE](#)].
- [15] F. Denef and M.R. Douglas, *Distributions of nonsupersymmetric flux vacua*, *JHEP* **03** (2005) 061 [[hep-th/0411183](#)] [[INSPIRE](#)].
- [16] D. Buttazzo et al., *Investigating the near-criticality of the Higgs boson*, *JHEP* **12** (2013) 089 [[arXiv:1307.3536](#)] [[INSPIRE](#)].
- [17] ATLAS collaboration, *Measurement of the top quark mass in the $t\bar{t} \rightarrow \text{lepton} + \text{jets}$ channel from $\sqrt{s} = 8$ TeV ATLAS data and combination with previous results*, *Eur. Phys. J. C* **79** (2019) 290 [[arXiv:1810.01772](#)] [[INSPIRE](#)].
- [18] CMS collaboration, *Measurement of the top quark mass using proton-proton data at $\sqrt{s} = 7$ and 8 TeV*, *Phys. Rev. D* **93** (2016) 072004 [[arXiv:1509.04044](#)] [[INSPIRE](#)].
- [19] CDF and D0 collaborations, *Combination of CDF and D0 results on the mass of the top quark using up to 9.7 fb^{-1} at the Tevatron*, [arXiv:1608.01881](#) [[INSPIRE](#)].
- [20] PARTICLE DATA GROUP collaboration, *Review of particle physics*, *PTEP* **2020** (2020) 083C01 [[INSPIRE](#)].
- [21] G.F. Giudice, P. Paradisi and A. Strumia, *Indirect determinations of the top quark mass*, *JHEP* **11** (2015) 192 [[arXiv:1508.05332](#)] [[INSPIRE](#)].
- [22] G. Corcella, R. Franceschini and D. Kim, *Fragmentation uncertainties in hadronic observables for top-quark mass measurements*, *Nucl. Phys. B* **929** (2018) 485 [[arXiv:1712.05801](#)] [[INSPIRE](#)].
- [23] S. Ferrario Ravasio, P. Nason and C. Oleari, *All-orders behaviour and renormalons in top-mass observables*, *JHEP* **01** (2019) 203 [[arXiv:1810.10931](#)] [[INSPIRE](#)].
- [24] S. Argyropoulos and T. Sjöstrand, *Effects of color reconnection on $t\bar{t}$ final states at the LHC*, *JHEP* **11** (2014) 043 [[arXiv:1407.6653](#)] [[INSPIRE](#)].
- [25] J. Reuter et al., *Exclusive top threshold matching at lepton colliders*, *PoS ICHEP2018* (2019) 654 [[arXiv:1811.03950](#)] [[INSPIRE](#)].
- [26] M. Boronat et al., *Top quark mass measurement in radiative events at electron-positron colliders*, *Phys. Lett. B* **804** (2020) 135353 [[arXiv:1912.01275](#)] [[INSPIRE](#)].
- [27] LCC PHYSICS WORKING GROUP collaboration, *Tests of the Standard Model at the International Linear Collider*, [arXiv:1908.11299](#) [[INSPIRE](#)].
- [28] TLEP DESIGN STUDY WORKING GROUP collaboration, *First look at the physics case of TLEP*, *JHEP* **01** (2014) 164 [[arXiv:1308.6176](#)] [[INSPIRE](#)].

- [29] K. Mönig, *High-precision α_s measurements from LHC to FCC-ee*, in *Proceedings, high-precision α_s measurements from LHC to FCC-ee: Geneva, Switzerland, 2–13 October 2015*, D. d’Enterria and P.Z. Skands eds., CERN, Geneva, Switzerland (2015) [[INSPIRE](#)].
- [30] D. d’Enterria, *α_s status and perspectives (2018)*, *PoS DIS2018* (2018) 109 [[arXiv:1806.06156](#)] [[INSPIRE](#)].
- [31] FCC collaboration, *FCC physics opportunities: Future Circular Collider conceptual design report volume 1*, *Eur. Phys. J. C* **79** (2019) 474 [[INSPIRE](#)].
- [32] T. Sen, *Fermilab site filler*, in *Accelerators for a Higgs factory (HF2012)*, *Fermilab Site Filler* (2012).
- [33] E. Gianfelice-Wendt, *Overview of Fermilab “SiteFiller” and LEP3*, in *Snowmass Agorà on e^+e^- circular colliders*, (2022).
- [34] A. Blondel and F. Zimmermann, *A high luminosity e^+e^- collider in the LHC tunnel to study the Higgs boson*, [arXiv:1112.2518](#) [[INSPIRE](#)].
- [35] A. Blondel et al., *LEP3: a high luminosity e^+e^- collider to study the Higgs boson*, [arXiv:1208.0504](#) [[INSPIRE](#)].
- [36] PARTICLE DATA GROUP collaboration, *Quantum chromodynamics, update* (2021).
- [37] G.P. Lepage, P.B. Mackenzie and M.E. Peskin, *Expected precision of Higgs boson partial widths within the standard model*, [arXiv:1404.0319](#) [[INSPIRE](#)].
- [38] D. d’Enterria et al., *The strong coupling constant: state of the art and the decade ahead*, [arXiv:2203.08271](#) [[INSPIRE](#)].
- [39] M. Cepeda et al., *Report from working group 2: Higgs physics at the HL-LHC and HE-LHC*, *CERN Yellow Rep. Monogr.* **7** (2019) 221 [[arXiv:1902.00134](#)] [[INSPIRE](#)].
- [40] V.S. Fadin and V.A. Khoze, *Threshold behavior of heavy top production in e^+e^- collisions*, *JETP Lett.* **46** (1987) 525 [*Pisma Zh. Eksp. Teor. Fiz.* **46** (1987) 417] [[INSPIRE](#)].
- [41] V.S. Fadin and V.A. Khoze, *Production of a pair of heavy quarks in e^+e^- annihilation in the threshold region*, *Sov. J. Nucl. Phys.* **48** (1988) 309 [*Yad. Fiz.* **48** (1988) 487] [[INSPIRE](#)].
- [42] M.J. Strassler and M.E. Peskin, *The heavy top quark threshold: QCD and the Higgs*, *Phys. Rev. D* **43** (1991) 1500 [[INSPIRE](#)].
- [43] A.H. Hoang and T. Teubner, *Top quark pair production at threshold: complete next-to-next-to-leading order relativistic corrections*, *Phys. Rev. D* **58** (1998) 114023 [[hep-ph/9801397](#)] [[INSPIRE](#)].
- [44] K. Melnikov and A. Yelkhovsky, *Top quark production at threshold with $O(\alpha_s^2)$ accuracy*, *Nucl. Phys. B* **528** (1998) 59 [[hep-ph/9802379](#)] [[INSPIRE](#)].
- [45] A.H. Hoang, A.V. Manohar, I.W. Stewart and T. Teubner, *The threshold $t\bar{t}$ cross-section at NNLL order*, *Phys. Rev. D* **65** (2002) 014014 [[hep-ph/0107144](#)] [[INSPIRE](#)].
- [46] F. Bach et al., *Fully-differential top-pair production at a lepton collider: from threshold to continuum*, *JHEP* **03** (2018) 184 [[arXiv:1712.02220](#)] [[INSPIRE](#)].
- [47] M. Beneke, Y. Kiyo, A. Maier and J. Piclum, *Near-threshold production of heavy quarks with $Q\bar{Q}$ threshold*, *Comput. Phys. Commun.* **209** (2016) 96 [[arXiv:1605.03010](#)] [[INSPIRE](#)].
- [48] M. Beneke, A. Maier, T. Rauh and P. Ruiz-Femenia, *Non-resonant and electroweak NNLO correction to the e^+e^- top anti-top threshold*, *JHEP* **02** (2018) 125 [[arXiv:1711.10429](#)] [[INSPIRE](#)].

- [49] M. Beneke, *A quark mass definition adequate for threshold problems*, *Phys. Lett. B* **434** (1998) 115 [[hep-ph/9804241](#)] [[INSPIRE](#)].
- [50] F. Simon, *A first look at the impact of NNNLO theory uncertainties on top mass measurements at the ILC*, in *International workshop on future linear colliders*, (2016) [[arXiv:1603.04764](#)] [[INSPIRE](#)].
- [51] M. Vos et al., *Top physics at high-energy lepton colliders*, [arXiv:1604.08122](#) [[INSPIRE](#)].
- [52] CLICDP collaboration, *Top-quark physics at the CLIC electron-positron linear collider*, *JHEP* **11** (2019) 003 [[arXiv:1807.02441](#)] [[INSPIRE](#)].
- [53] F. Simon, *Scanning strategies at the top threshold at ILC*, in *International workshop on future linear colliders*, (2019) [[arXiv:1902.07246](#)] [[INSPIRE](#)].
- [54] FCC collaboration, *FCC-ee: the lepton collider. Future Circular Collider conceptual design report volume 2*, *Eur. Phys. J. ST* **228** (2019) 261 [[INSPIRE](#)].
- [55] *CLIC beam-beam interactions documentation: reduced charge option*, https://clic-beam-beam.web.cern.ch/clic-beam-beam/350gev_l6_bx8mm_f19550.html.
- [56] S. Poss and A. Sailer, *Luminosity spectrum reconstruction at linear colliders*, *Eur. Phys. J. C* **74** (2014) 2833 [[arXiv:1309.0372](#)] [[INSPIRE](#)].
- [57] K. Seidel, F. Simon, M. Tesar and S. Poss, *Top quark mass measurements at and above threshold at CLIC*, *Eur. Phys. J. C* **73** (2013) 2530 [[arXiv:1303.3758](#)] [[INSPIRE](#)].
- [58] G. Bernardi et al., *The Future Circular Collider: a summary for the U.S. 2021 Snowmass process*, [arXiv:2203.06520](#) [[INSPIRE](#)].
- [59] X.C. Lou, *Circular electron-positron collider — status and progress*, talk at HKUST-IAS, 17 January 2022.
- [60] *CEPC webpage*, <http://cepc.ihep.ac.cn>.
- [61] M. Zanetti, *Beamstrahlung at circular e^+e^- Higgs factories*, [HF2012](#), (2012).
- [62] T. Sen, *An e^+e^- storage ring Higgs factory at Fermilab*, talk at *Accelerators for a Higgs factory workshop*, 14–16 November 2012.
- [63] J. Wenninger, *Lepton collider overview*, talk at *Future Circular Collider study kickoff meeting*, <https://indico.cern.ch/event/282344/timetable>, (2014).
- [64] F. Zimmermann, *High-energy physics strategies and future large-scale projects*, *Nucl. Instrum. Meth. B* **355** (2015) 4 [[INSPIRE](#)].
- [65] A. Grassellino et al., *Unprecedented quality factors at accelerating gradients up to 45 MVm^{-1} in niobium superconducting resonators via low temperature nitrogen infusion*, *Supercond. Sci. Technol.* **30** (2017) 094004 [[arXiv:1701.06077](#)] [[INSPIRE](#)].
- [66] J.P. Delahaye et al., *Muon colliders*, [arXiv:1901.06150](#) [[INSPIRE](#)].
- [67] *The international muon collider collaboration webpage*, <https://muoncollider.web.cern.ch>.
- [68] M.S. Berger, *The top-anti-top threshold at muon colliders*, *AIP Conf. Proc.* **435** (1998) 797 [[hep-ph/9712486](#)] [[INSPIRE](#)].
- [69] R.B. Palmer, *Muon colliders*, *Rev. Accel. Sci. Tech.* **7** (2014) 137 [[INSPIRE](#)].
- [70] Y. Alexahin et al., *Muon collider Higgs factory for Snowmass 2013*, in *Community summer study 2013: Snowmass on the Mississippi*, (2013) [[arXiv:1308.2143](#)] [[INSPIRE](#)].